Engineering Note

Accelerator Division

Mechanical Support Department

Teamcenter Identifier: ED0000569

Date: 02/19/13

Title: LBNE Horn 1 Inner Conductor Cooling Test Study

Authors(s): Cory Crowley

Summary:

The Long Baseline Neutrino Experiment (LBNE) will be utilizing the identical inner and outer conductor designs for Horn 1 and Horn 2 as designed for the NuMI/NOvA experiment. As part of the R&D phase for this project, and to assure that the Finite Element Analysis (FEA) which will be completed for this task is accurate, an inner conductor cooling test was deemed necessary.

Prior conductor cooling tests had been performed, with the goal of determining a realistic heat transfer coefficient to be applied in an analysis. These tests however, resulted in a wide range of data which was hindered by an unacceptable level of experimental error. The repeat of this test was required to provide the same data at a higher level of confidence, by reducing measurement uncertainty through the use of more accurate equipment and higher temperature variations that far exceed the possible measurement errors.

This data will then be used to apply varying heat transfer coefficients to a thermo-mechanical analysis, based on the specific geometry of the conductor and the cooling spray nozzles in use. By obtaining accurate heat transfer coefficients, the goal of providing design information such as maximum temperatures, stresses, deformations, and fatigue life with a high degree of confidence can be achieved.

Table of Contents

III. Requirements and Specifications

1. Scope of work includes the design and fabrication of a cooling nozzle test stand to be used for the purposes of investigating heat transfer coefficients on the Horn 1 neck region. The goal is to determine with a high degree of confidence, the heat transfer coefficients to be used on the Horn 1 Inner Conductor, as well as complete an uncertainty analysis on the data obtained.
2. Milestones are:
   A. Cart Fabrication Complete
   B. Horn Nominal Operation Test Complete
   C. Horn Improved Operational Test Complete
3. Test stand construction must follow all NEPA enclosure codes for electrical safety due to the close proximity of pressurized water tubing.
4. ES&H and QA requirements are: See item #3.
5. Functional and design requirements are such that:
   A. Spray test cart must provide adequate water pressure and flow to potentially feed eight (8) 1 GPM nozzles @ 40 PSI.
   B. Temperature measurement devices must be embedded in inner conductor sample tube, to achieve accurate temperature readings.
   C. Supply water temperature must be 20 C, as is defined in the analysis.
   D. Power supplied to the test fixture must match that of the anticipated power which will be put into the conductor during operation. If sufficient power cannot be applied to the test, results must be scaled to the theoretical operating parameters and this must be clearly shown.
6. There are no interface requirements for this system, other than it must utilize electrical connections and utilities commonly available at the MI-8 service building.
7. Acceptance criteria are successful test runs using the originally specified nozzles which provide valid test data with a high degree of certainty. Possible additional test runs may be made to improve cooling coefficient.
8. Safe and proper functioning characteristics include utilizing basic electrical safety and LOTO procedures while making setup changes.
9. The test fixture and test procedure do not warrant a formal design review

IV. Engineering Risk Assessment

Engineering Risk		
Item	Risk Element	Risk Assessment
A	Technology	1
B	Environmental Impact	1
C	Vendor Issues	2
D	Resource Availability	2
E	Quality Requirements	1
F	Safety	2
G	Manufacturing Complexity	1
Project Management Risk		
Item	Risk Element	Risk Assessment
H	Schedule	3
I	Interfaces	1
J	Experience / Capability	1
K	Requlatory Requirements	1
L	Project Funding	2
M	Project Reporting Requirements	1
N	Public Impact	1
O	Project Cost	1

Table 3.1 Engineering & Project Management Risk

Engineering Risk Element										
Chapter	A	B	C	D	E	F	G	High Risk	Total	
1	1	1				2		>10	4	
3	1	1		2	1	2		>16	7	
4	1	1	2		1	2	1	>19	8	
5	1	1	2		1	2	1	>19	8	
6		1		2	1	2	1	>16	7	
7	1				1	2	1	>13	5	
8						2		>4	2	
9		1				2		>7	3	
Project Risk Element										
	H	I	J	K	L	M	N	O	High Risk	Total
Score	3	1	1	1	2	1	1	1	>25	11

Table 3.2 Engineering and Project Risk Elements

V. System Design

1. Major Components & Equipment
    - Heating element outer shell (Analog Horn Neck):
      1” OD X .750” ID X 20” long 6061-T6 uncoated aluminum tube.
    - Heating Element:
      Omega CIR Series High Watt Density Cartridge Heater; 5000W model, P/N: CIR5205/240V.
    - Analog Horn Neck Thermocouples (At Neck Region):
      Omega TJC36 Compact Series Thermocouple Probes, P/N: TJC48-CPSS-020G-6, Type T
    - Analog Horn Neck Thermocouples (At Ends):
      Omega TJC36 Compact Series Thermocouple Probes, P/N: TJC48-CPSS-062G-6, Type T
    - Thermocouple Readout:
      Omega Panel Mount Thermometer for Type T Thermocouples, P/N: DP302-TC2
    - Thermocouple Jack Panel:
      Omega P/N: 19MJP1-10-T-OSW-MTR
    - Variable Input Switch:
      Omega Rotary Selector Switch, P/N: OSW3-10
    - Power Supply:
      5000W, 240V Single Phase Input VARIAC Potentiometer.
    - Experimentation Cart:
      McMaster-Carr P/N: 2826T53
    - Gear Pump:
      McMaster-Carr P/N: 4272K21
    - Flow Meter:
      McMaster-Carr P/N: 41995K43
    - Pressure Gauges:
      McMaster-Carr P/N: 4003K71 0-60 Range
    - 16 Gal Reservoir Tank:
      McMaster-Carr P/N: 4439T14
    - Water Temperature Thermocouple:
      McMaster-Carr P/N: 3872K37 Type T
    - Water Filter:
      McMaster-Carr P/N: 9860K11
    - Volt Meter:
      Fluke 179 True RMS Multimeter
    - Amp Meter:
      Fluke 334A 600 AMP Digital Clamp Meter
    - NOvA Design Spray Nozzles:
      Spraying Systems Co. H1/8VV-SS11005
    - Increased Capacity Nozzles:
      Spraying Systems Co. H1/8VV-SS11006

Spray test cylinder construction consisted of a cast acrylic tube, with flat end plates glued on for ease of mounting to the test cart. The tube OD was 12”, and the effective test length was 20” end plate to end plate. With a wall thickness of .25”, the ID was 11.5” which was a close representation to the actual outer conductor ID utilized on the horns. The end plates of the cylinder are equipped with inspection and cleaning ports, as well as removable center tube bushings for installation and removal of the inner conductor neck test piece.

The entire assembly was supported by angle iron that was bolted to the test cart to provide for a rigid testing apparatus. This attachment method also promoted easy fitment of supply and return lines to the spray test cylinder. Fabrication drawings are attached as an addendum to this note.

2. P & ID

The process layout is an iteration of what was done previously to complete this test. Changes were made to better facilitate cooling of the reservoir tank and to reduce equipment needs. The P & ID diagram can be seen below:

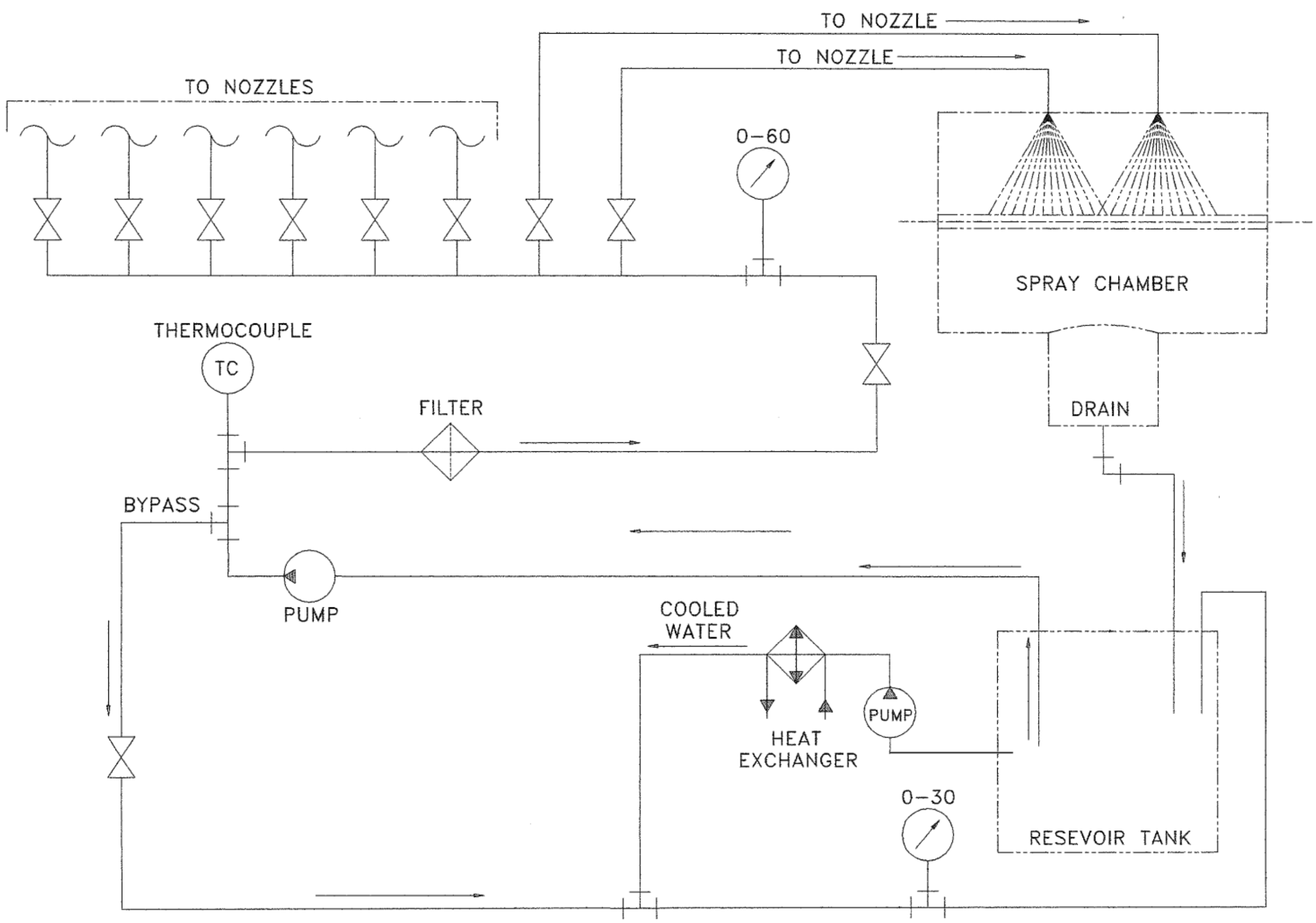

Figure 4.2.1 Horn Cooling Water Spray Test Supply Diagram

3. Spray Test Setup

The spray test setup was built to duplicate the current horn design and nozzle placement, as the initial plan is to utilize the existing spray ports for nozzle testing. Area of interest in is the neck region of the horn, and figure 4.3.1 outlines the location of the horn this test is based on. It can also be seen in the figure the distribution of nozzles around the circumference of the outer conductor, which has them placed at 120 degree intervals.

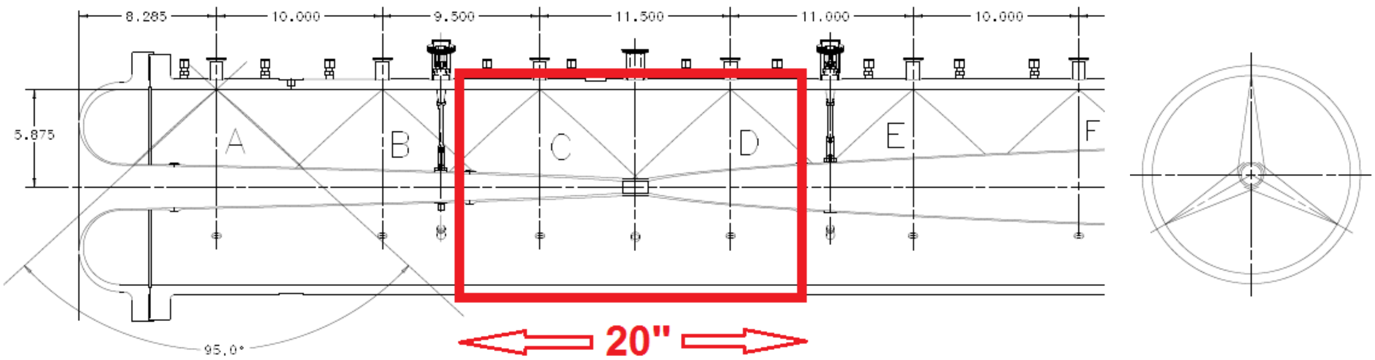

Figure 4.3.1 Horn 1 Cooling Test Region

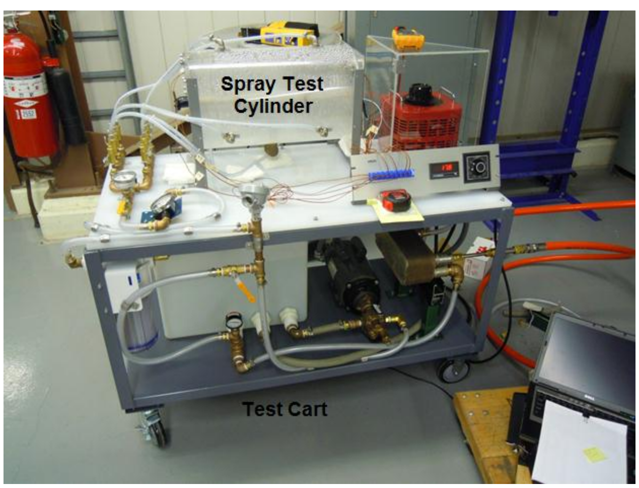

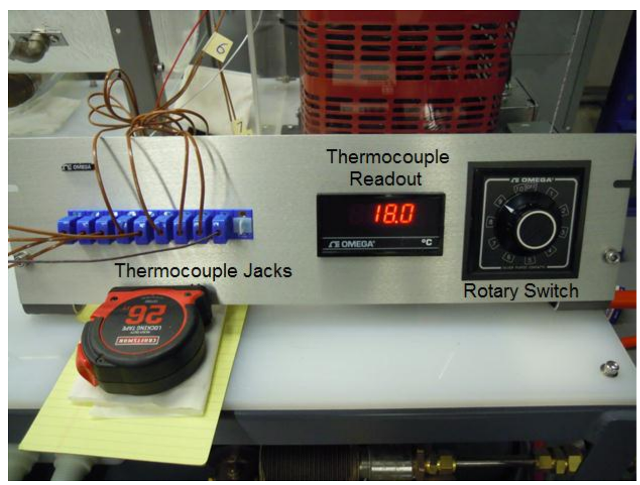

Figures 4.3.2 & 4.3.3 Spray Test Setup

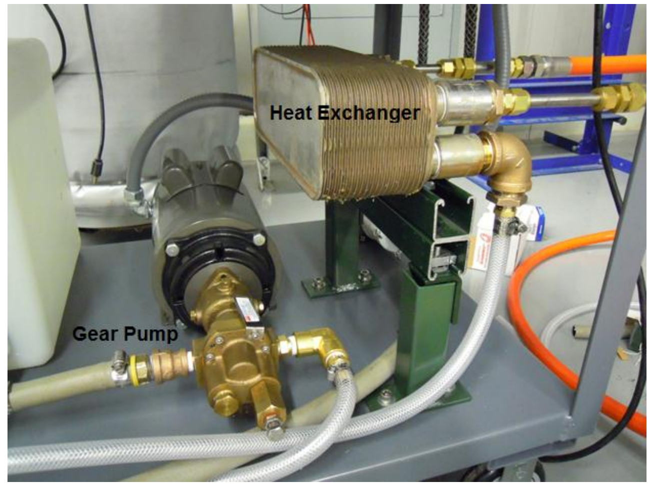

Figures 4.3.4 & 4.3.5 Spray Test Setup

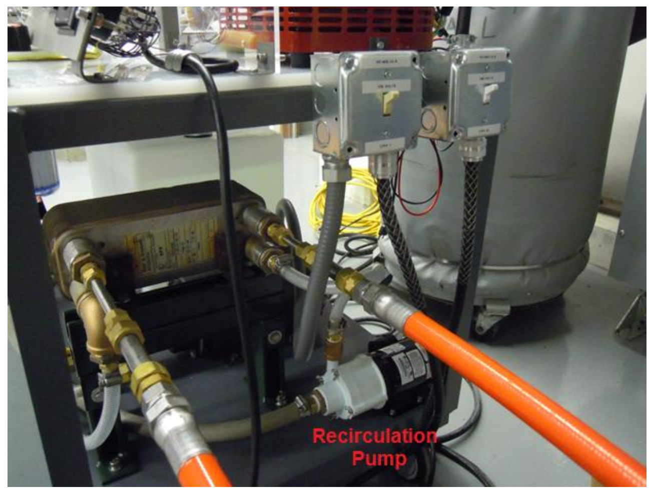

Figures 4.3.6 & 4.3.7 Spray Test Setup

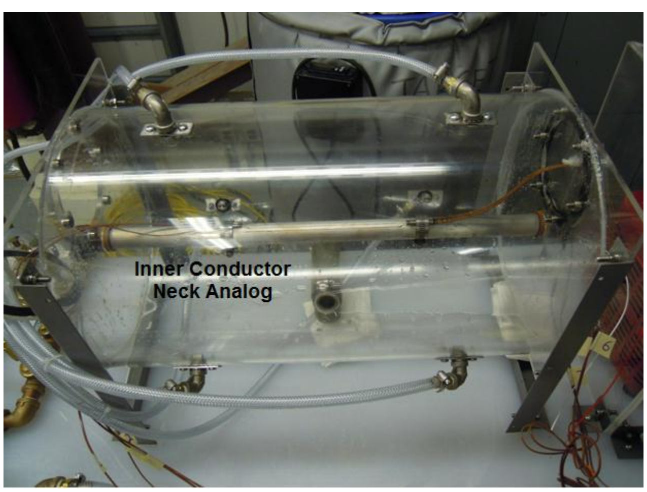

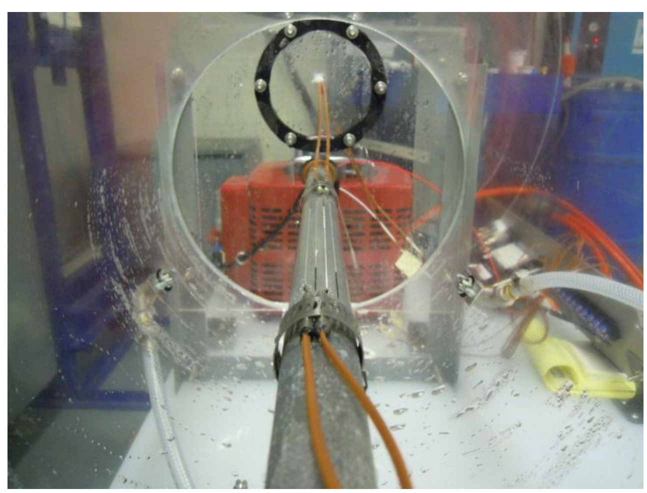

Figures 4.3.8 & 4.3.9 Spray Test Setup

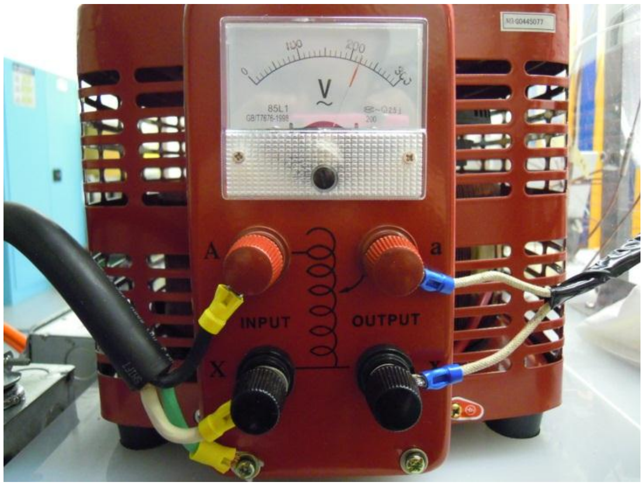

Figures 4.3.10 & 4.3.11 Spray Test Setup

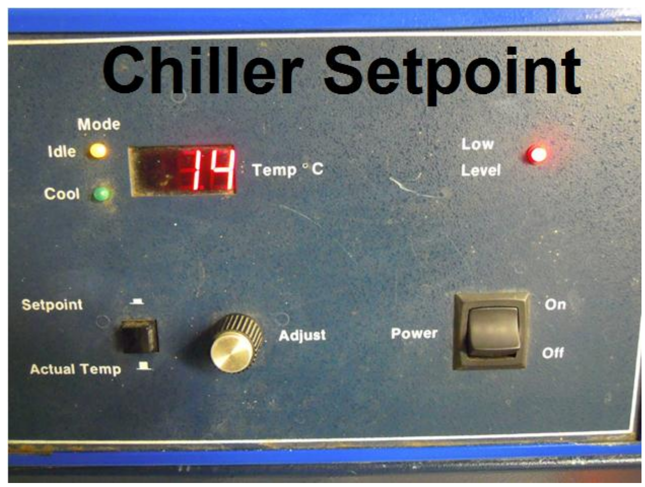

Figures 4.3.12 & 4.3.13 Spray Test Setup

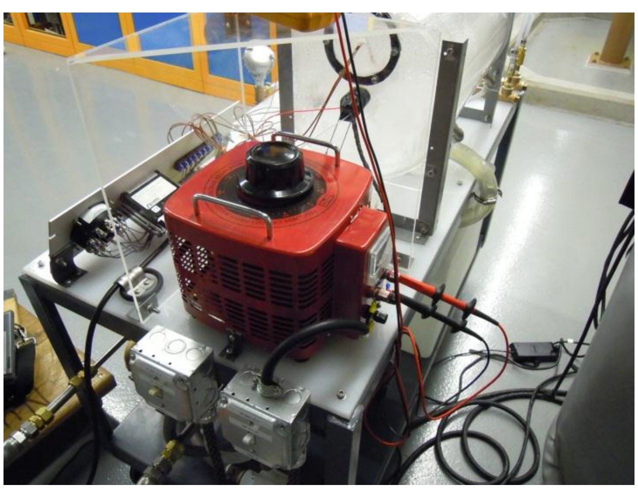

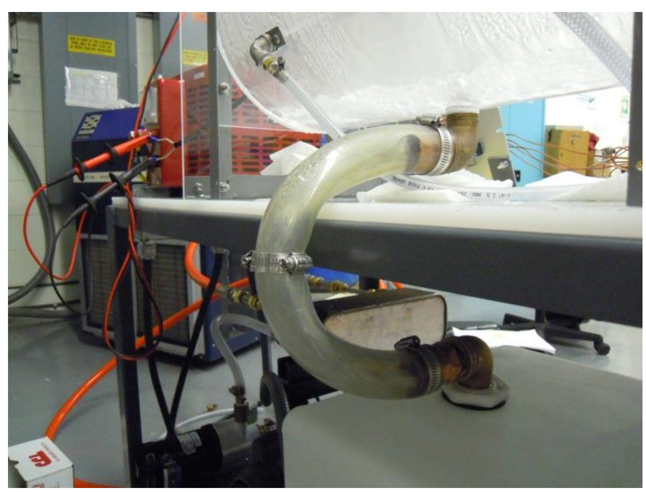

Figures 4.3.14 & 4.3.15 Spray Test Setup

As can be seen from the figures above, the entire test apparatus is on a single cart for maximum portability. Not shown however, is an external heat exchanging unit, used to provide cooled water to the cart-mounted exchanger which in-turn cools the 16 Gallon reservoir. This indirect cooling approach proved to be successful in that it provided long time durations before the spent cooling water temperature started to affect the supply water temperature. A result of this characteristic was that thermocouple temperatures could be gathered in a single run, without waiting for temperatures to re-stabilize after data recording.

4. Thermocouple Placement

Placement of thermocouples is of the utmost importance for this test, as the cooling coefficients determined are directly impacted by the accuracy of the thermocouples. If the thermocouples are poorly bonded to the conductor analog, or have a disproportionate amount of cooling relative to what the surrounding material receives, a great deal of experimental error is introduced and the findings have a low degree of confidence. To ensure that the readings taken accurately represented the surrounding material temperatures, each thermocouple was set in a slot or hole and embedded in epoxy. This method assured that no cooling water spray came in direct contact with a thermocouple, disproportionately affecting the readings.

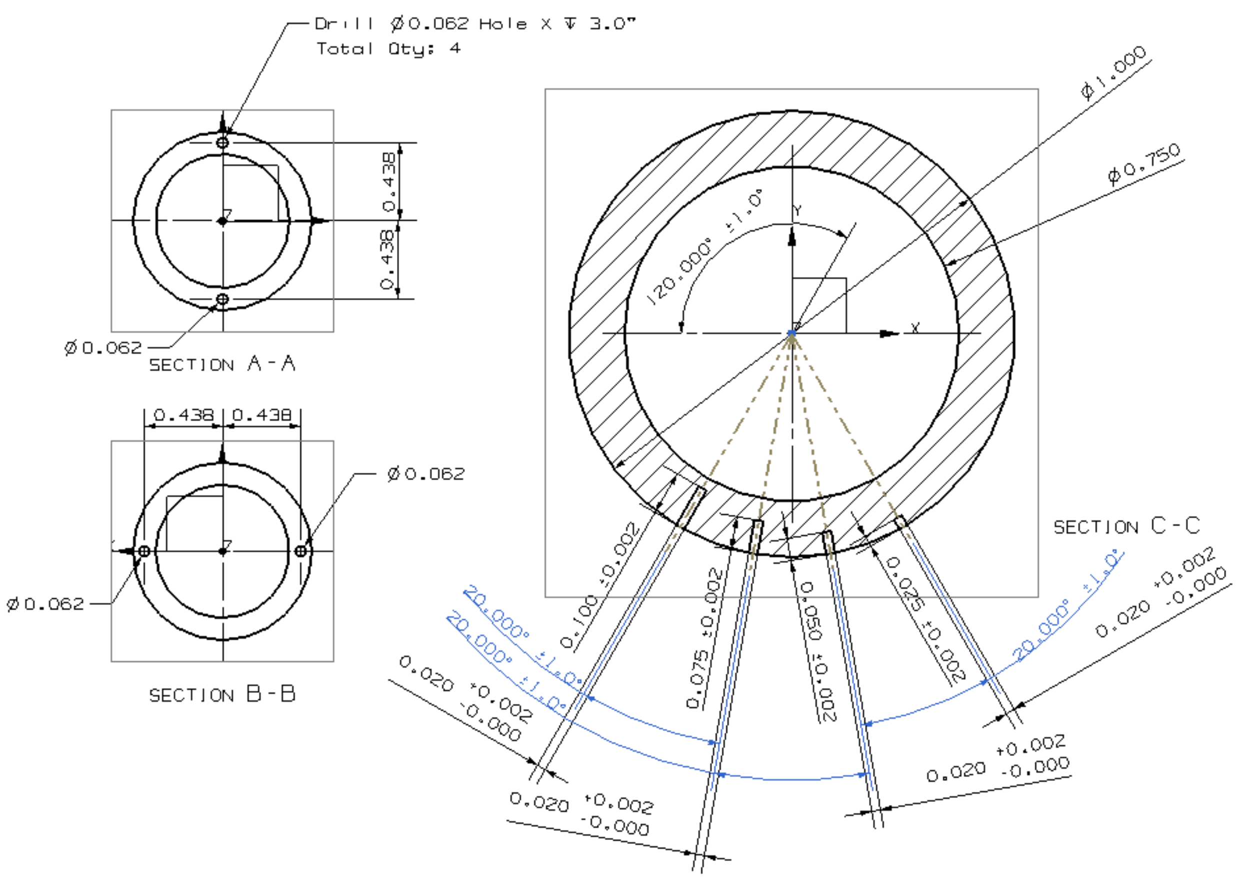

Figure 4.4.1 Cut-outs for Thermocouple Placement

One aspect of the test that was desired was to understand how the interface between the spray pattern and geometry of the tube affected operational temperatures. To achieve this, a total of eight (8) thermocouples were embedded in the tube body, all with different positions relative to the spray pattern. Two (2) thermocouples were placed across from each other on either end of the tube, with both sides offset 90 degrees from one another. The remaining 4 thermocouples were placed at the neck region, where this test was mainly focused, and positioned at varying depths, ranging from .100” deep to just .025” away from the top surface. These locations are shown in the figures below:

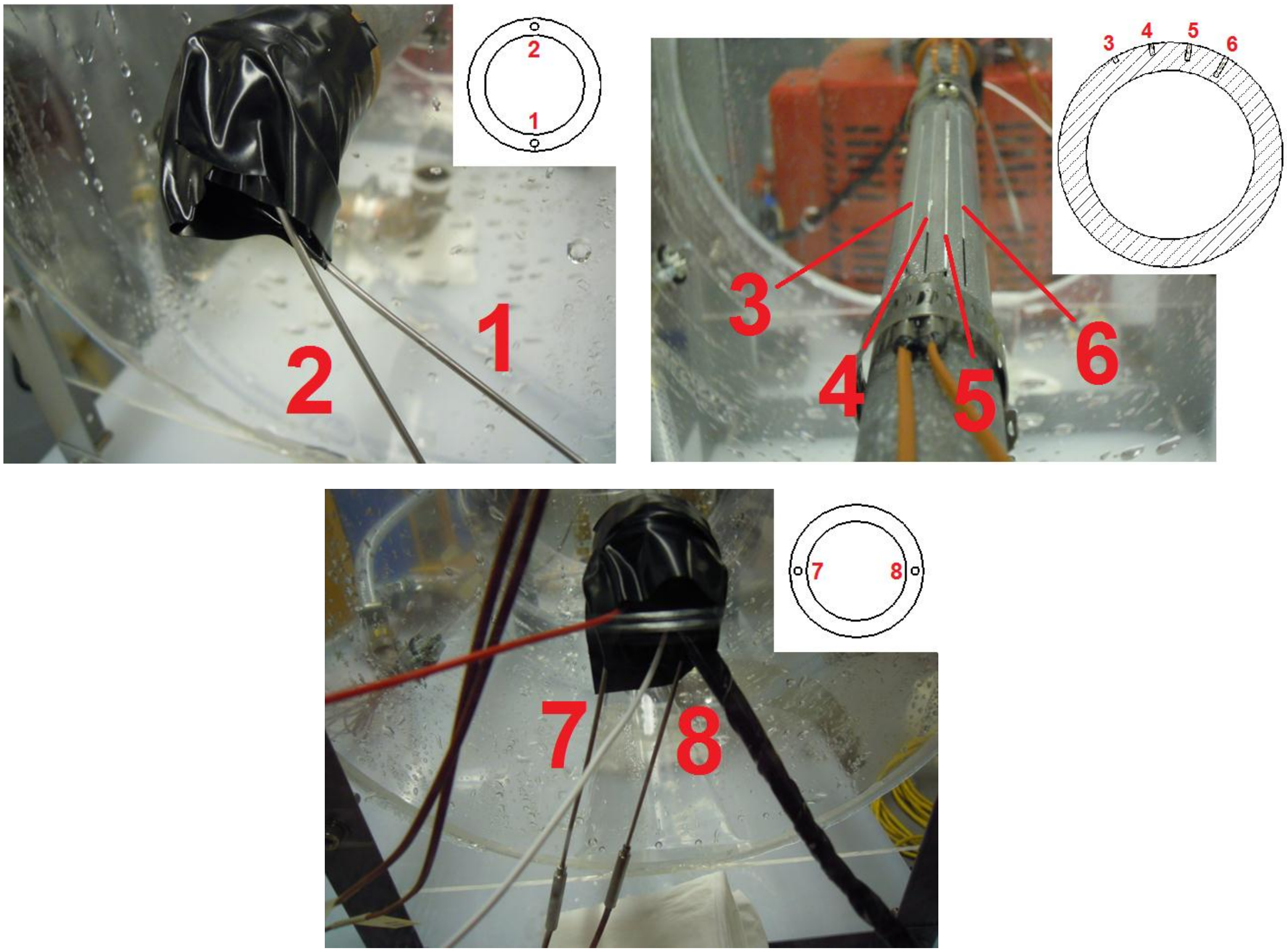

Figures 4.4.2, 4.4.3, & 4.4.4 Thermocouple Locations

The main area of interest is the neck location at the center of the spray test. The four .020” O.D. thermocouples placed in this region will determine the highest achievable film coefficient based on the spray nozzles selected and flow parameters given. This area of the horn has the highest stresses and is very temperature dependent. The combined power from beam energy deposition and resistive heating from the current pulse determine the final temperature. All efforts to reduce this will yield lower stresses with a higher fatigue life, which increases operational efficiency.

VI. Horn 1 Neck Heating Calculations for Analog Aluminum Cylinder

1. Power Input Through Beam Energy Deposition

The inner conductor operating temperature is due in part to the beam energy deposition that occurs in the material. It depends on material properties, geometry, and proximity to the beam. The test was done using an inner conductor neck analog, and so the geometry does not precisely match that of an actual horn. That being said, the geometry very closely represents a finished conductor neck, and the calculations done for the test piece, as well as the results, should closely agree with those for the actual component.

An energy deposition analysis was completed by Byron Lundberg, utilizing the following parameters listed below:

Protons Per Pulse	4.9 X 10^13
Proton Beam Pulse Width	10 µs
Beam Energy	120 GeV
Beam Power to Target	708 kW
Beam Sigma	1.3 mm
Target Fin Width	7.4 mm
Beam pulse repetition rate	1.33 seconds
Current Pulse Width	2.1 ms
Current	230 kA
Target Position in Horn 1	-35 cm [LE-0]

Figure 6.1.1 E-Dep Analysis Parameters

The resultant energy deposition in the Neck region of horn 1 was found to be = 1.59×10^{-3} GeV/g

Density of aluminum is listed at: $2.7 g/cm^3$

Volume of the inner conductor analog (1" OD X .125 Wall X 20" L) is = $(\pi r_1^2 - \pi r_2^2)*L$

$= (\pi(.5in)^2 - \pi(.375in)^2)*20in = 6.87223in^3$

$6.87223in^3 = .000113m^3$

Equation to solve for power from beam heating =

$((ED \times 1.60217646 \times 10^{-19} \times 4.9 \times 10^{13} \times 1 \times 10^{9})/1.33) \times 2700000$ (With 6061-T6 aluminum neck)

Plugging in 1.59×10^{-3} GeV/g into ED, the result is $2.53405 \times 10^{7}\ W/m^3$

By taking the power deposited per unit volume and multiplying by the calulcated volume listed above, the result is: $((2.53405 \times 10^{7}\ W/m^3) \times (.000113m^3))=$ **2,863.48 W** over the 20" length of the inner condcutor test piece.

2. Power Input Through Resistive Heating

The second component of the inner conductor operating temperature is due to the resistive heating it undergoes during a current pulse. The resistive heating depends upon the cross-sectional area of the conductor, the resistivity, as well as the current being transmitted. As with the above calculation on beam energy deposition, the geometry of the test piece will yield a slightly different result than the actual conductor. This result however, will also closely agree with the real component.

A SPICE simulation was completed by Ken Bourkland, showing the current pulse parameters below:

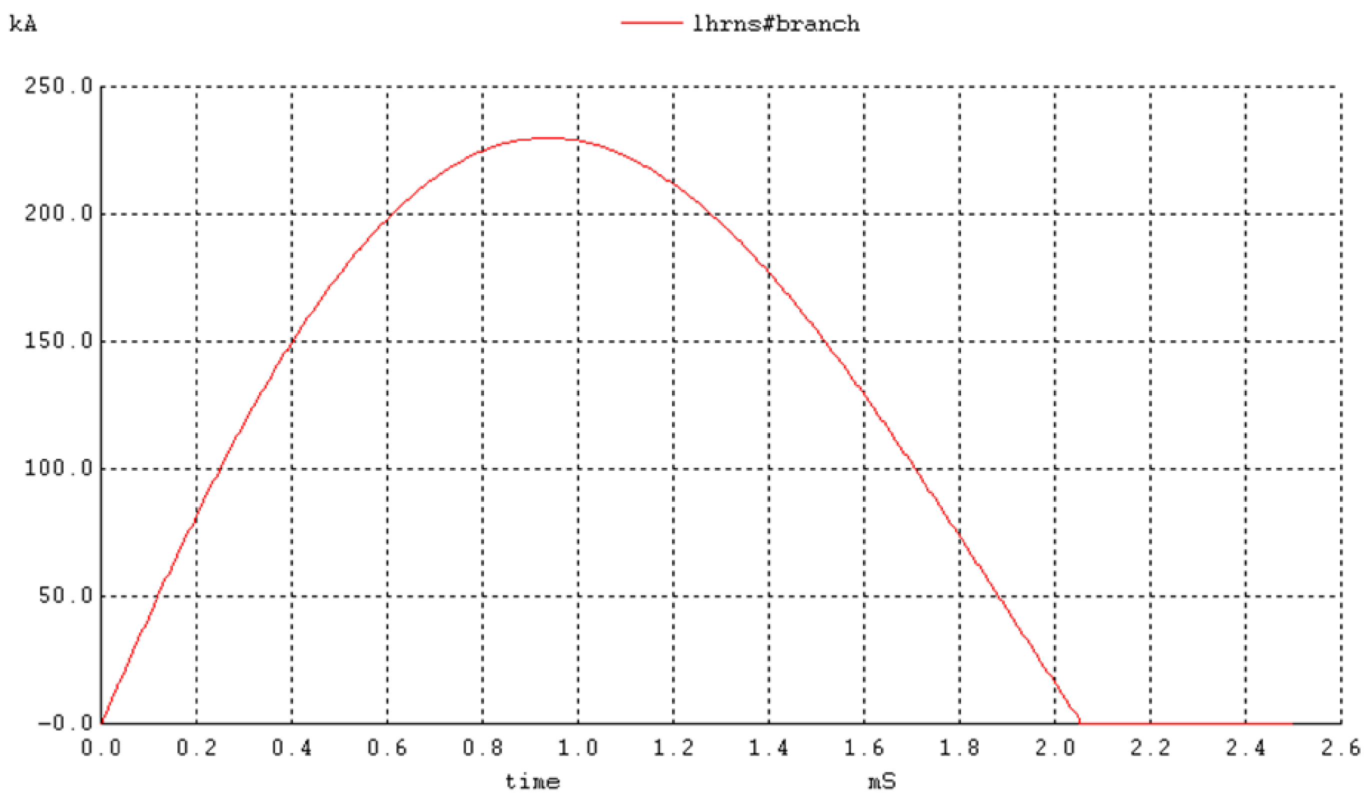

SPICE simulation: Pulse width = 2.058ms. Current Peak occurs at 935uS

Figure 6.2.1 SPICE Simulation Results

The current pulse width was found to be = 2.058ms The peak current is set to = 230kA

Resistivity of aluminum is estimated to be = 4.5×10^{-8} Ohm-m at the average expected operational temperatures (60 C).

Equation to solve for power from beam heating =

$$\frac{(((\text{Resistivity}) \times (\text{Peak Current})^2 \times (\text{Pulse Width}))}{(2 \times (2\pi \times (\text{Mid-Radius of Wall}) \times (\text{Wall Thickness}))^2 \times 1.33))}$$

Replacing the variables with known values, the equation yields:

$$\frac{(((4.5 \text{ X } 10^{-8} \text{ Ohm-m}) \text{ X } (230\text{kA})^2 \text{ X } (.002058))}{(2 \text{ X } (2\pi \text{ X } (.01111) \text{ X } (.003175))^2 \text{ X} 1.33))} = \underline{3.74936 \text{ X } 10^7 \text{ W/m}^3}$$

By taking the power deposited per unit volume and multiplying by the volume, the result is: ((3.74936 X 10^7 W/m^3) X (.000113m^3))= **4,236.77 W** over the 20" length of the inner condcutor test piece.

The combined heating load from the beam energy deposition and resistive heating that would duplicate operational conditions on Horn 1 neck region in the LBNE beamline is 2,863.48 W + 4,236.77 W **=** **7,100.25 W** over the 20" length of the inner condcutor test piece.

3. Determination of heat Transfer Coefficient

Solving for the heat transfer coefficient is based off the following equation:

Q = h X A(s) X (Ts – Tw), where:

Q = Energy into System
h = Convection Coefficient
A(s) = Surface Area
Ts = Surface Temperature of Heated Tube
Tw = Temperature of Cooling Water Spray

This equation can be re-arranged to solve for h, yielding:

h = Q/A(s) X (Ts – Tw)

Area of the tube is also known, given by: (Tube OD) X π X (Tube Length) = .0254m X π X .508m = .0405m^2

Water input temperature is kept to 20 C, leaving the only open variable, Ts, to be recorded from the various thermocouples during testing.

The input power to re-create operational conditions was calculated to be 7,100.25 W; however the limitations of the cartridge heating element and power supply used in the test will only allow a power input of roughly 4000 W. This is inconsequential however, as the cooling coefficient is not dependent on input power. The power and resultant temperatures scale linearly, and so the results of the test can simply be multiplied by a factor of (7,100.25 / 4000) = **1.78** to achieve theoretical operating temperatures. Obtaining the maximum power input available for the test was determined by measuring the voltage and current being fed into the heating element, and then simply using the equation:

Power (W) = Volts (V) X Current (I)

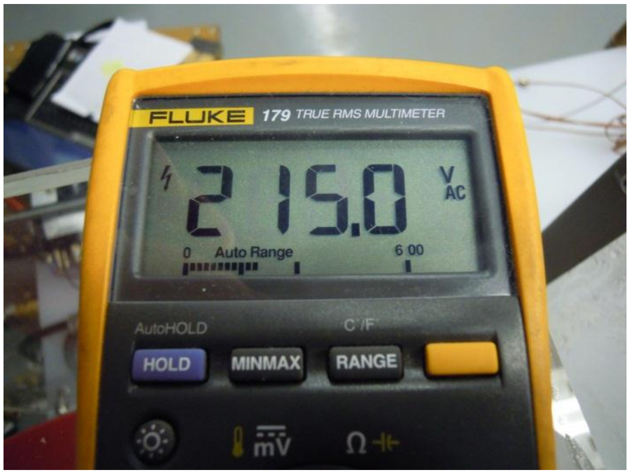

Figure 6.3.1 Heating Cartridge Voltage

Figure 6.3.2 Heating Cartrige Current

Plugging these values into W = V X I results in a power consumption of: 215V X 18.6A = 3,999W ~ **4kW**

VII. Nozzle Testing Utilizing NOvA Design

1. Nozzle Type & Parameters

The current horn design utilizes a flat spray nozzle on the neck region, due to optimum coverage for that specific geometry. Nearly all of the water droplets make direct contact with the conductor, and so overspray is not an issue. These nozzles, coupled with their 120 Degree azimuthal placement, also provide nearly complete coverage of the inner conductor neck. Because of this, this pattern of nozzle is nearly ideal for the type of spray coverage required. An example of the nozzle can be seen below:

VeeJet Spray Nozzles,
Standard Spray, Small Capacity
H1/8VV-316SS11005

Ordering Number	H1/8VV-316SS11005
Nozzle Prefix Code	H
Nozzle Type Prefix	VV
Nozzle Inlet Connection	Male NPT
Spray Angle	110
Spray Pattern Type	Tapered Edge
Capacity @ 40 psi	0.5
Nozzle Type	H-VV
Inlet Connection	1/8
Capacity Size	$\boxed{5}$
Material	316 Stainless Steel
Material Code	316SS
Length	0.875
Hex	0.5
Net Wt. (oz)	0.5
Capacity Data	*Click here*
Coverage/ Distribution Data	*Click here*
Drop Size Data	*Click here*
Option	Integral Strainer
Minimum PSI	5
Maximum PSI	500

Figure 7.1.1 NOvA Style VeeJet Flat Spray Nozzle; 0.5 GPM @ 40 PSI

2. Results

The first tests were completed utilizing the nominal design shown above, and data points were obtained at various pressures and flow rates. This data was used to determine the average convection coefficient for the entire tube, for the neck region only, as well as the anticipated operating temperature of the neck region. Recorded data can be seen in the following figures:

	Startup Temperature	Running at 30 PSI & 2.6 GPM	Running at 40 PSI & 3 GPM	Running at 50 PSI & 3.25 GPM	Running at 60 PSI & 3.5 GPM
Water Temperature =	20	20	20	20	20
Thermocouple 1 =	18.2	38.2	36.7	35.6	34.3
Thermocouple 2 =	18.2	36.3	34.9	33.7	32.6
Thermocouple 3 =	18.2	34.3	32.9	31.6	30.6
Thermocouple 4 =	18.3	35.6	33.7	32.3	31.2
Thermocouple 5 =	18.4	34.6	32.9	31.5	30.4
Thermocouple 6 =	18.4	37.1	35.3	33.9	32.9
Thermocouple 7 =	18.1	41.6	39.6	38.9	36.6
Thermocouple 8 =	17.9	39.3	38.1	36.5	35.4

Figure 7.2.1 H1/8VV-316SS11005 Nozzle Results

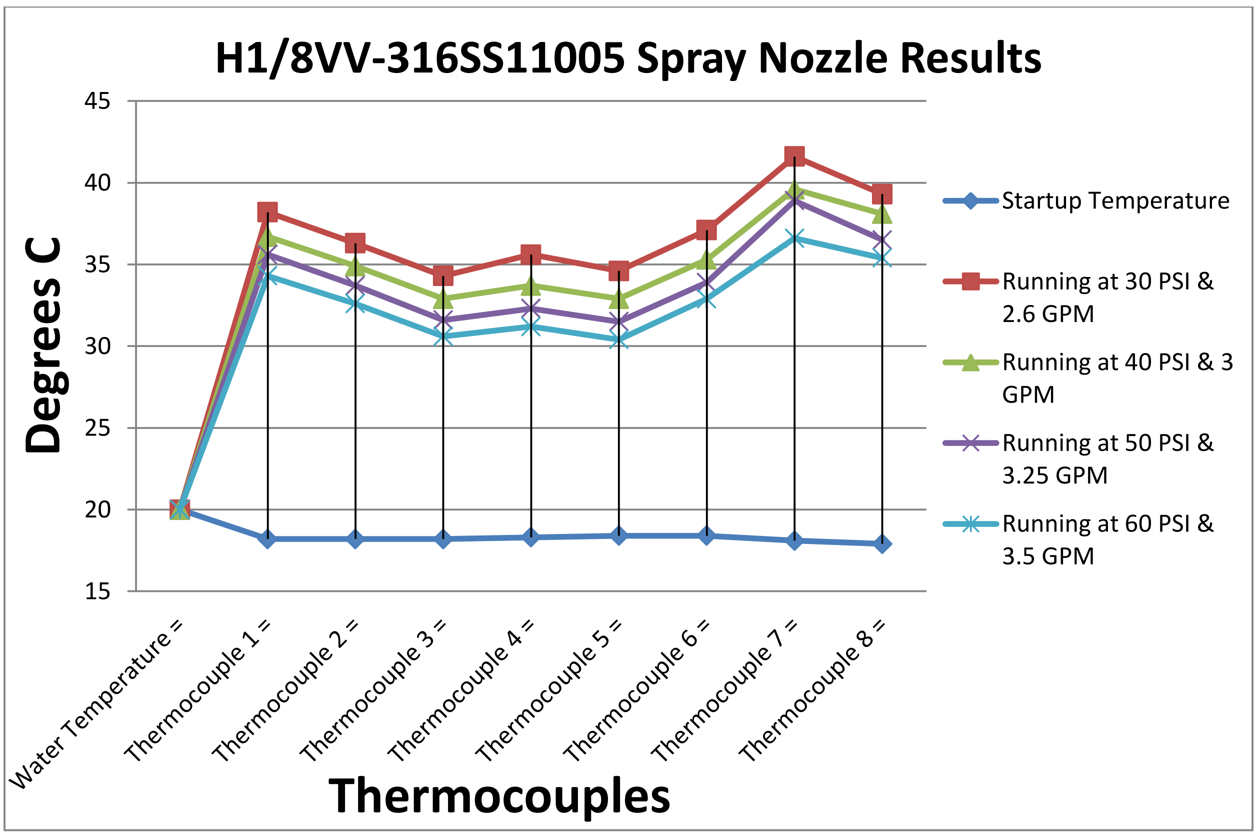

Figure 7.2.2 H1/8VV-316SS11005 Nozzle Results

Using the data obtained, we can solve for all values of interest. For reference purposes, the thermocouples embedded in the neck region are outlined in red.

	Startup Temperature	Running at 30 PSI & 2.6 GPM	Running at 40 PSI & 3 GPM	Running at 50 PSI & 3.25 GPM	Running at 60 PSI & 3.5 GPM
Water Temperature =	20	20	20	20	20
Thermocouple 1 =	18.2	38.2	36.7	35.6	34.3
Thermocouple 2 =	18.2	36.3	34.9	33.7	32.6
Thermocouple 3 =	18.2	34.3	32.9	31.6	30.6
Thermocouple 4 =	18.3	35.6	33.7	32.3	31.2
Thermocouple 5 =	18.4	34.6	32.9	31.5	30.4
Thermocouple 6 =	18.4	37.1	35.3	33.9	32.9
Thermocouple 7 =	18.1	41.6	39.6	38.9	36.6
Thermocouple 8 =	17.9	39.3	38.1	36.5	35.4
Average Thermocouple Temperature	18.2	37.1	35.5	34.3	33.0
Average Delta T	N/A	17.1	15.5	14.3	13.0
Average Convection Coefficient W/m^2-C	N/A	5765.9	6365.2	6929.2	7595.4
Estimated Steady State Temperature (With 1.78 Power Correction Factor)	N/A	50.5	47.6	45.4	43.1
Average Thermocouple Temperature For Neck Region	18.3	35.4	33.7	32.3	31.3
Average Delta T For Neck Region	N/A	15.4	13.7	12.3	11.3
Average Convection Coefficient W/m^2-C For Neck Region	N/A	6411.7	7207.4	8011.4	8757.5
Estimated Steady State Temperature (With 1.78 Power Correction Factor) For Neck Region	N/A	47.4	44.4	41.9	40.1

Figure 7.2.3 Heat Transfer Coefficients & Estimated Operating Temperatures for .5 Capacity Nozzle

VIII. Nozzle Testing Utilizing Increased Capacity Nozzles

1. Nozzle Type & Parameters

The alternate design tested is of the same style currently used on the neck region in the NOvA design, however the capacity is increased slightly to allow for a greater flow rate at the same operating pressures. As with the previous nozzle, nearly all of the water droplets make direct contact with the conductor.

VeeJet Spray Nozzles,
Standard Spray, Small Capacity
H1/8VV-316SS11006

Ordering Number	H1/8VV-316SS11006
Nozzle Prefix Code	H
Nozzle Type Prefix	VV
Nozzle Inlet Connection	Male NPT
Spray Angle	110
Spray Pattern Type	Tapered Edge
Capacity @ 40 psi	0.6
Nozzle Type	H-VV
Inlet Connection	1/8
Capacity Size	6
Material	316 Stainless Steel
Material Code	316SS
Length	0.875
Hex	0.5
Net Wt. (oz)	0.5
Capacity Data	*Click here*
Coverage/ Distribution Data	*Click here*
Drop Size Data	*Click here*
Option	Integral Strainer
Minimum PSI	5
Maximum PSI	500

Figure 8.1.1 NOvA Style VeeJet Flat Spray Nozzle; 0.6 GPM @ 40 PSI

It should be noted however that one aspect of testing which is not easily determined is the effect of higher flow rates & pressures on the water film thickness that surrounds the inner conductor neck region during operation. It was determined from previous studies that a film thickness of approximately 1mm was acceptable when utilizing the .5 capacity nozzles at the rated pressure of 40 PSI. This thickness was determined based of the beam interaction angle with the water, which affect the outcome of the Monte Carlo results.

Upon further discussion with LBNE physicists, it was decided that the 1mm requirement for film thickness could be relaxed; further analysis supporting this is ongoing. Additional studies on this topic aside, testing utilizing the higher capacity nozzle at a various range of pressures did not seem to drastically increase the water film around the neck region. From an educated guess during the various test runs and observations from viewing through the clear test cell, is it estimated that film thickness increased no more than 20% from the nominal flow parameters of the .5 capacity nozzles at 30 PSI & 2.6 GPM. This topic is discussed further at the conclusion of this report.

2. Results

	Startup Temperature	Running at 30 PSI & 3.1 GPM	Running at 40 PSI & 3.6 GPM	Running at 50 PSI & 4 GPM	Running at 60 PSI & 4.4 GPM
Water Temperature =	20	20	20	20	20
Thermocouple 1 =	18.2	35	34	33.1	32.3
Thermocouple 2 =	18.2	33	31.9	31	30
Thermocouple 3 =	18.2	33.8	32.1	31	29.9
Thermocouple 4 =	18.3	35	33.3	32.3	31.2
Thermocouple 5 =	18.4	33.8	32	30.9	29.8
Thermocouple 6 =	18.4	34.6	33	32.1	31.1
Thermocouple 7 =	18.1	35.9	34.4	33.9	32.9
Thermocouple 8 =	17.9	36.3	34.9	34	32.8

Figure 8.2.1 H1/8VV-316SS11006 Nozzle Results

It can clearly be seen, and is quite obvious from a theoretical perspective, that the higher capacity nozzles have a greater effect on the heat transfer coefficient at all pressure ranges when compared to the nominal design.

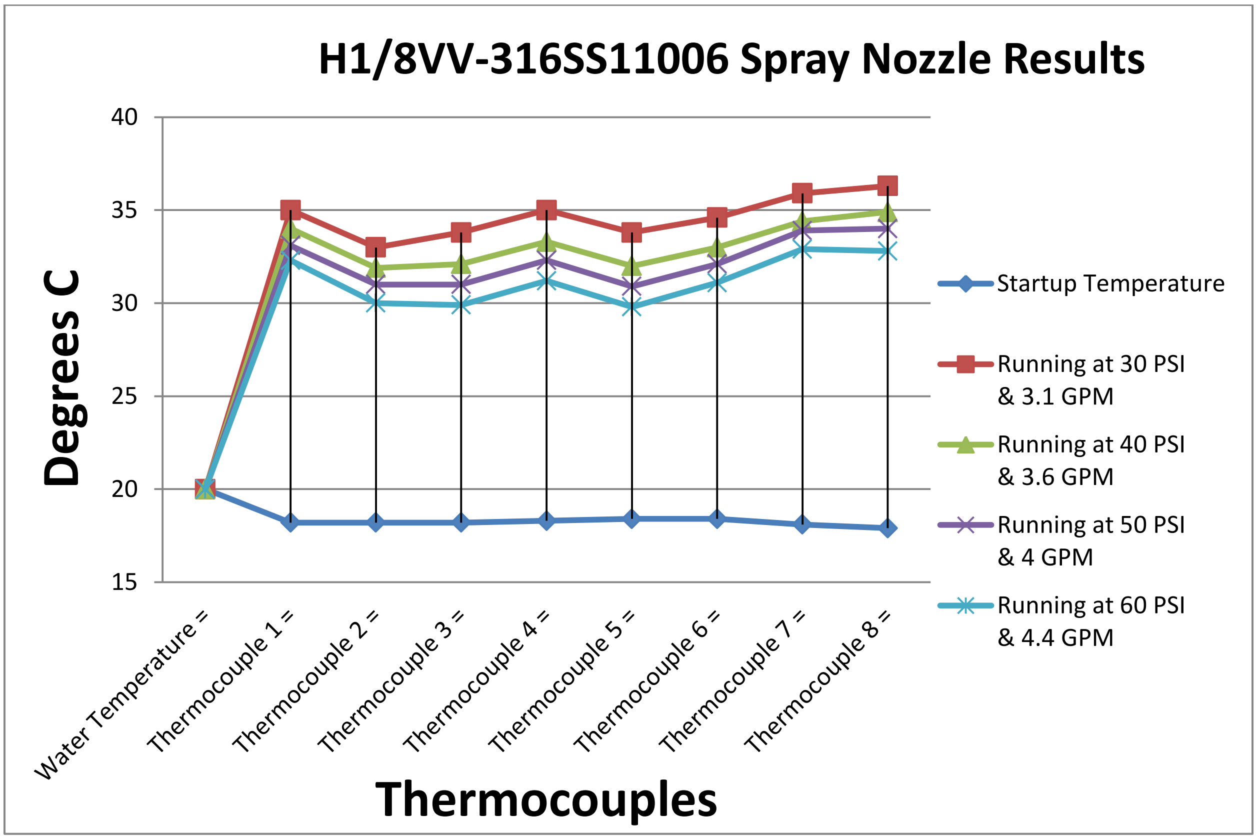

Figure 8.2.2. H1/8VV-316SS11006 Nozzle Results

	Startup Temperature	Running at 30 PSI & 3.1 GPM	Running at 40 PSI & 3.6 GPM	Running at 50 PSI & 4 GPM	Running at 60 PSI & 4.4 GPM
Water Temperature =	20	20	20	20	20
Thermocouple 1 =	18.2	35	34	33.1	32.3
Thermocouple 2 =	18.2	33	31.9	31	30
Thermocouple 3 =	18.2	33.8	32.1	31	29.9
Thermocouple 4 =	18.3	35	33.3	32.3	31.2
Thermocouple 5 =	18.4	33.8	32	30.9	29.8
Thermocouple 6 =	18.4	34.6	33	32.1	31.1
Thermocouple 7 =	18.1	35.9	34.4	33.9	32.9
Thermocouple 8 =	17.9	36.3	34.9	34	32.8
Average Thermocouple Temperature	18.2	34.7	33.2	32.3	31.3
Average Delta T	N/A	14.7	13.2	12.3	11.3
Average Convection Coefficient W/m^2-C	N/A	6728.5	7480.4	8035.9	8777.0
Estimated Steady State Temperature (With 1.78 Power Correction Factor)	N/A	46.1	43.5	41.9	40.0
Average Thermocouple Temperature For Neck Region	18.3	34.3	32.6	31.6	30.5
Average Delta T For Neck Region	N/A	14.3	12.6	11.6	10.5
Average Convection Coefficient W/m^2-C For Neck Region	N/A	6904.9	7836.6	8530.5	9403.9
Estimated Steady State Temperature (With 1.78 Power Correction Factor) For Neck Region	N/A	45.5	42.4	40.6	38.7

Figure 8.2.3 Heat Transfer Coefficients & Estimated Operating Temperatures for .6 Capacity Nozzle

IX. Water Film Measurement

A critical aspect of the cooling spray on the inner conductor is the thickness of the water film formed on the surface by coalescing water droplets. This water film effectively adds mass to the inner conductor, changing the interaction between the horn and the focused particles. The extent of this affect is unknown however, and additional modeling studies on horn sensitivity are on-going. It is a well-established goal, however, to maximize the cooling coefficient on the inner conductor while minimizing the film thickness. Understanding how strongly nozzle pressure and flow parameters relate to film thickness is important for future design considerations.

Prior cooling tests had attempted to determine the relationship between water film thickness and flow parameters of the nozzles, although visibility during a full pressure spray test is near zero. It was set as a goal for this experiment to re-attempt measuring the water film thickness, using more stable methods and improved observation techniques.

Figure 9.1 shows the measurement technique used to determine water film thickness on the neck region. A basic measurement tab was bonded to the surface directly under the top nozzle so as to provide minimal disturbance to the normal spray pattern. The prior cooling test carried out had an estimated film thickness of approximately 1mm with the nominal flow conditions at the horn of 30 PSIG.

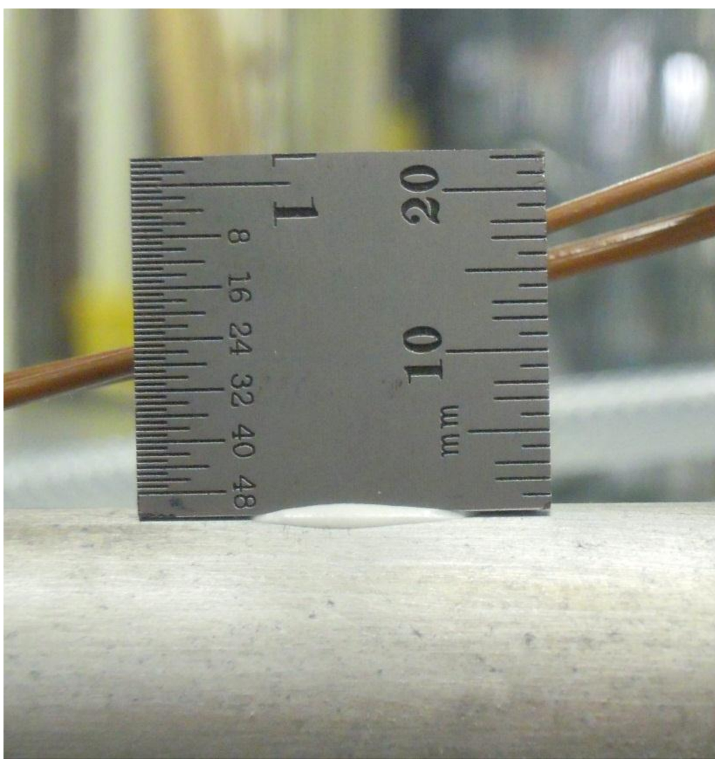

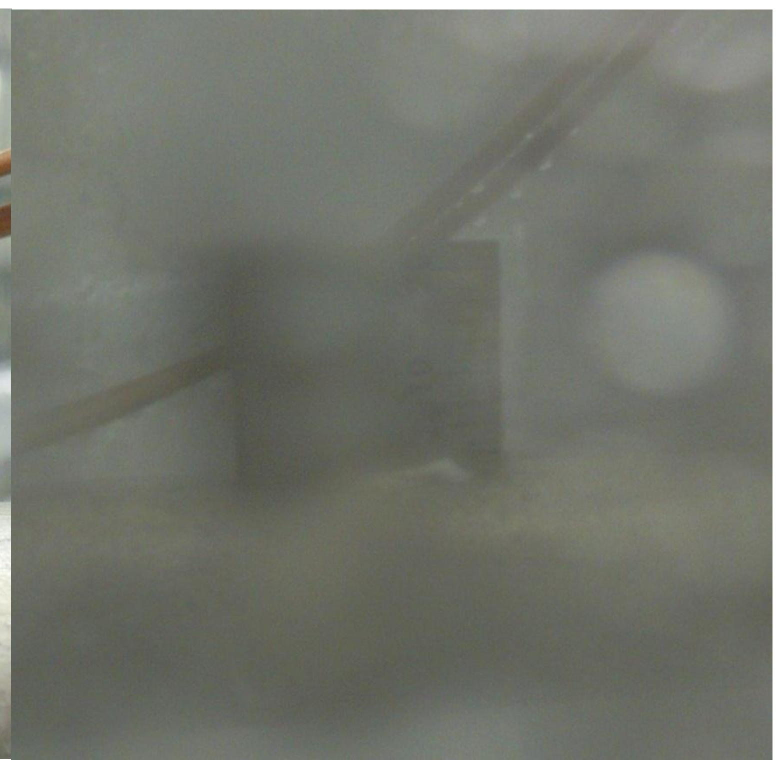

Figure 9.1 Film Test

Figure 9.2 Full Pressure Spray Test

After the test was started, it became evident that documenting the film thickness was awkward due to the massive amount of splash back from the spray which can be seen in figure 9.2. Viewing the test in person yielded clearer results however. It was seen that the actual film thickness regardless of the pressure or flow ranges tested always remained close to 0mm. Flow and pressure changes however, only affected the meniscus of the water in relation to the measuring tab itself.

Low pressures and flows yielded little interaction between the water spray and measuring tab, however as the flow increased, the water started to flow up the sides. Edited representations are illustrated below:

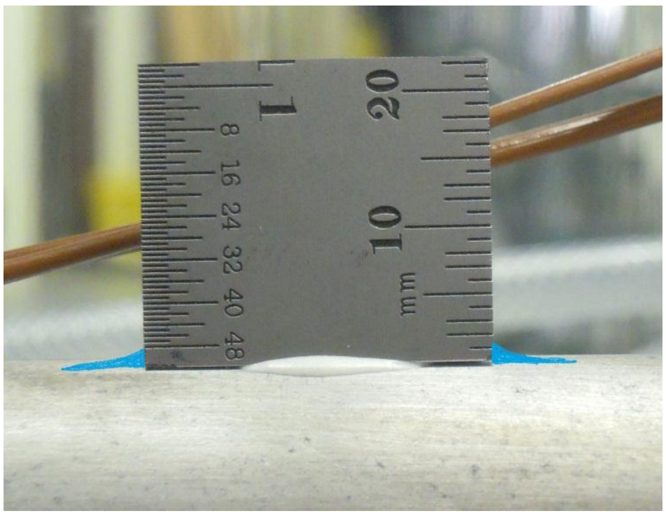

Figure 9.3 Low Pressure & Flow

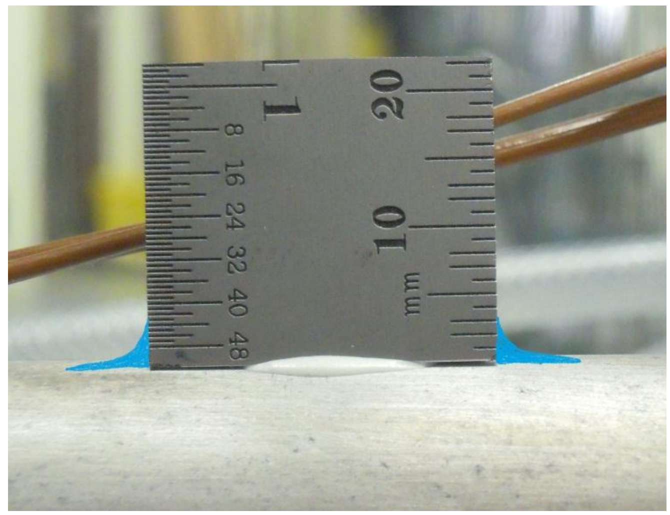

Figure 9.4 High Pressure & Flow

It was observed that most of the water spray, regardless of pressure or flow, bounced off the inner conductor analog and splashed back on to the outer conductor wall. This was visually confirmed, as changing to different nozzles and increasing pressures lead to more water washing down the sides. At no point could a visible film be identified other than on the edges of the water film test. These observations show that the water film thickness is confirmed to be no more than approximately 1mm, and most likely is less than that for all nozzles types and flow parameters tested.

One consideration however is that the higher flow rate will affect the amount of water dripping off the bottom of the horn, and as such, there will be an increase in water film thickness in that region. It is unknown however what the surface area of the thicker water film is, so it is not quantified in this study. It will however, be taken into consideration with the final nozzle choice.

XI. Conclusion

1. Nozzle Choice & Design Update

Based on previous assumptions of convection coefficients, the initial goal set forth for Horn 1 was to achieve 7,500 W/m^2-C in the neck region. This value would then be scaled to other areas of the conductor based on spray coverage and flow rates as outlined below:

Approximate Length along Horn Axis (cm)

	0-50cm	50cm-110cm	110cm – 210cm	210cm-300cm
Convective heat transfer Coefficient (h): ($W/m^2 \bullet C$)	6000	7500	6000	4500

These heat transfer coefficients were used in a preliminary analysis prior to CD-1 for the LBNE project and resulted in an acceptable range of steady state temperatures. It now remains as the current goal for the final horn design to meet these heat transfer values, pending completion of an in-depth thermal and structural analysis. The analysis and final heat transfer coefficient relationship is an iterative process and must be re-evaluated intermittently.

When looking at the available test data in figure 10.1.1 for the .5 capacity nozzles, it can be seen that at the normal operating pressure for the horn, which is 30 PSI, yields a convection coefficient at the neck just below 6,500 W/m^2-C.

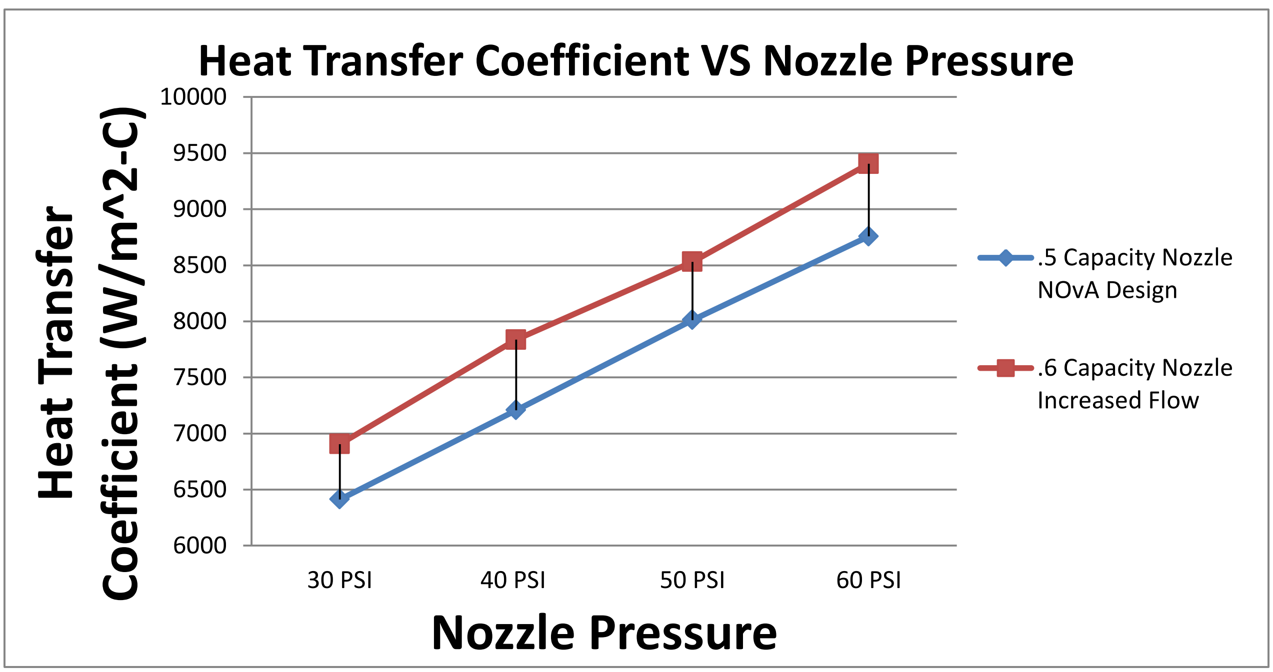

Figure 10.1.1 Pressure and Heat Transfer Comparisons of Tested Nozzles

This value does not currently meet the desired goal, and therefore two alternate flow parameters can be used to achieve the desired result by referencing Figure 10.1.1 and 10.1.2. The identified options based on nozzles tested are as follows:

A. Keep original nozzle design in place and increase operational pressures to 40 – 45 PSI.
B. Install higher capacity nozzle and operate at pressures of 35-40 PSI.

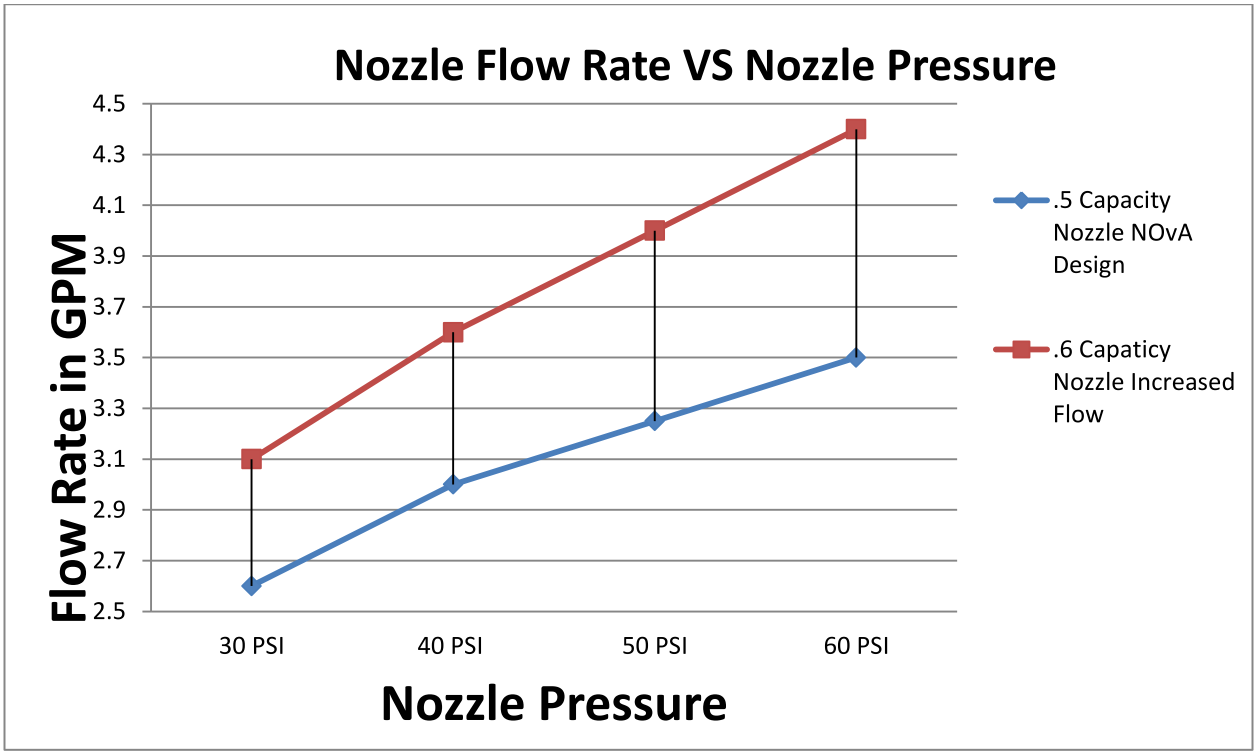

Figure 10.1.2 Flow Rate and Nozzle Pressure Comparisons of Tested Nozzles

<u>Option A</u> will involve increasing overall water flow rate to the horn by approximately 15%, and pressure by approximately 43%, based off flow increases observed in tested nozzles. It will also increase the water erosion rate of the inner conductor surface, as this has caused documented horn failures at different institutions in the past. There has not been an identifiable study however, that documents erosion rates of aluminum with varying pressure nozzles at different heights.

<u>Option B</u> will involve replacing the .5 capacity nozzles in six (6) locations with .6 capacity nozzles, followed by a modest increase in water pressure & flow to the horn. The estimated flow rate increase to the horn would be about 11%, with a corresponding pressure increase of approximately 22%. Option B will also add to the water film thickness on the horn neck, even more so than option A, however all nozzle testing yielded little discernible difference as opposed to nominal pressure and flow rate.

2. Recommended Heat Transfer Coefficients for Horn 1 Inner Conductor

Note* - This section was finalized during the LBNE Horn 1 conductor analysis that was completed by Ang Lee from PPD.

It was found through iterative analysis that keeping the original nozzle and flow parameters from the NOvA horn design could yield acceptable operating temperatures. Although the higher cooling coefficient goal of 7,500 at the neck region could be reached, it was determined the additional risk from water spray erosion and demand on the water tank suction pump did not validate a design change given the small temperature drop it would have provided. This could not be known until the analysis was completed and results reviewed.

Therefore, the maximum cooling coefficient in the neck region was set at 6500/7500 = 86.7% of prior analysis parameters. The cooling coefficients used in the analysis are listed below:

Approximate Length along Horn Axis (cm)

	0-50cm	50cm-110cm	110cm – 210cm	210cm-300cm
Convective heat transfer Coefficient (h): ($W/m^2 \bullet C$)	5200	6500	5200	3900